An Equivalent Modeling Method for the Radiated Electromagnetic Interference of PCB Based on Near-field Scanning

Yin-Shuang Xiao [1], Dan Ren [2], Pei Xiao [1], and Ping-An Du [1*]

[1] School of Mechanical and Electrical Engineering
University of Electronic Science and Technology of China, Chengdu 611731, China
xiaoyinshuang@qq.com, xiaopei_uestc@sina.cn, dupingan@uestc.edu.cn*

[2] Institute of Electronic Engineering
China Academy of Engineering Physics, Mianyang 621900, China
rendan_uestc@163.com

Abstract ─ Since the structure complexity of a PCB makes its EMI modeling be very difficult or impossible, an equivalent modeling method to predict the electromagnetic radiation of a PCB is presented by means of a dipole array based on near-field scanning. Firstly, the equivalent modeling method is theoretically derived and its accuracy is validated by a commercial full-wave tool. Then, the equivalent model is applied to predict the electromagnetic coupling of different parts on a PCB and the electromagnetic leakage of a PCB in an enclosure with numerous small apertures. The results show that the proposed method has high efficiency and acceptable accuracy.

Index Terms ─ Dipole array, electromagnetic interference, equivalent modeling, printed circuit board (PCB), near-field scanning.

I. INTRODUCTION

The printed circuit board (PCB) is the most frequently-used component in electronic device. Since the PCB always radiates electromagnetic interference while working, it is necessary to model the PCB during the electromagnetic compatibility (EMC) analysis of an electronic device. However, the complexity of the structure of PCB makes its EMI modeling be very difficult and time-consuming, even impossible. Thus, investigation of the equivalent model with a simpler structure and similar EMI characteristics of the original PCB is of significance in applications [1-4].

In the EMC analysis area of PCB, Shi and Weng analyzed the electromagnetic emission information of PCB by near-field scanning, and the equivalent electric/ magnetic current source was applied to replace radiation characteristics of original source [5-6]. This method showed a good performance on far-field radiation characteristic prediction, but was not fit to represent near-field electromagnetic radiation and coupling characteristics. The optimizing work of equivalent model and dipole-dielectric-conducting plane (DDC) model which simultaneously considered the affection of dielectric slab and ground plane have been introduced by Tong [7-9]. Then Obiekezie proposed new equivalent dipole models, which predicted the EMI characteristic of 3D radiation source on the finite ground plane and characterized edge currents along a finite ground plane [10-11]. In [12], an equivalent modeling method without phase information was realized by using particle swarm optimization algorithm. The outer components, like heat sink structure and IC pins were considered in [13-15], and practical equivalent dipole models were established. A decomposition method was proposed to predict the coupling from a digital noise to the radio frequency (RF) antenna based on equivalent dipole modeling method and reciprocity theory in [16-18].

In this paper, an equivalent dipole modeling method of PCB is proposed, which can predict the near-field electromagnetic radiation characteristics of original PCB model, and validated by patch antenna with a commercial full-wave tool. Then, an improved analytical algorithm is established, and the efficiency of this algorithm is verified by calculating the coupling parameters of different parts of PCB and antenna array. Finally, the equivalent model is applied to predict the electromagnetic leakage of the PCB in an enclosure with numerous small apertures, and also shows very high accuracy.

II. EQUIVALENT MODELING METHOD

A. Basic theory

According to the basic theory of electromagnetic [19], the near field PCB radiated is quasi-static. It includes abundant radiation information of PCB. So it is

Submitted On: October 8, 2018
Accepted On: January 18, 2019

workable to make use of this critical information to establish the equivalent model of the PCB. On the other hand, the real radiating source on the PCB are onboard electric and magnetic current. They have similar radiating characteristics with electric and magnetic dipole. Therefore, electric and magnetic dipole are adaptable to be used to build the equivalent model we need.

In this paper, the magnetic near field is extracted by HFSS simulation, which includes three Cartesian components: H_x, H_y, and H_z. Correspondingly, the magnetic dipole is chosen to constitute the equivalent model of a PCB, which can be decomposed into three moment components: M_x, M_y, and M_z. As a result, the radiation characteristics of the equivalent model are mainly determined by the dipole and its image source of ground plane (GND). The dipole is located far away from the boundary of GND, so the edge diffraction is ignored. Besides, according to the image theory, the radiation of vertical magnetic moment can be ignored when the dipole is laid close to GND. So only tangential moment components M_x and M_y are considered.

When a dipole is located in (x_0, y_0, z_0), the magnetic field of point (x, y, z) in free space which is radiated by M_x, M_y and their image sources can be expressed as [18]:

$$\begin{aligned} H_x &= a_{H_x}^{M_x} M_x + a_{H_x}^{M_y} M_y \\ &= \frac{k_0^2 M_x}{4\pi}\Big[-\frac{(y-y_0)^2+(z-z_0)^2}{r_1^2} g_1(r_1) + g_2(r_1) \\ &\quad -\frac{(y-y_0)^2+(z-z_0+2h)^2}{r_2^2} g_1(r_2) + g_2(r_2)\Big] \\ &\quad + \frac{k_0^2 M_y}{4\pi}\Big[\frac{(x-x_0)(y-y_0)}{r_1^2} g_1(r_1) + \frac{(x-x_0)(y-y_0)}{r_2^2} g_1(r_2)\Big], \end{aligned} \tag{1a}$$

$$\begin{aligned} H_y &= a_{H_y}^{M_x} M_x + a_{H_y}^{M_y} M_y \\ &= \frac{k_0^2 M_x}{4\pi}\Big[\frac{(x-x_0)(y-y_0)}{r_1^2} g_1(r_1) + \frac{(x-x_0)(y-y_0)}{r_2^2} g_1(r_2)\Big] \\ &\quad + \frac{k_0^2 M_y}{4\pi}\Big[-\frac{(x-x_0)^2+(z-z_0)^2}{r_1^2} g_1(r_1) + g_2(r_1) \\ &\quad -\frac{(x-x_0)^2+(z-z_0+2h)^2}{r_2^2} g_1(r_2) + g_2(r_2)\Big], \end{aligned} \tag{1b}$$

$$\begin{aligned} H_z &= a_{H_z}^{M_x} M_x + a_{H_z}^{M_y} M_y \\ &= \frac{k_0^2 M_x}{4\pi}\Big[\frac{(x-x_0)(z-z_0)}{r_1^2} g_1(r_1) + \frac{(x-x_0)(z-z_0+2h)}{r_2^2} g_1(r_2)\Big] \\ &\quad \frac{k_0^2 M_y}{4\pi}\Big[\frac{(y-y_0)(z-z_0)}{r_1^2} g_1(r_1) + \frac{(y-y_0)(z-z_0+2h)}{r_2^2} g_1(r_2)\Big], \end{aligned} \tag{1c}$$

where h is the thickness of the PCB, r_1 r_2, $g_1(r)$, $g_2(r)$ are respectively defined as:

$$r_1 = \sqrt{(x-x_0)^2+(y-y_0)^2+(z-z_0)^2}, \tag{2a}$$

$$r_2 = \sqrt{(x-x_0)^2+(y-y_0)^2+(z-z_0+2h)^2}, \tag{2b}$$

$$g_1(r) = \frac{e^{-jk_0 r}}{r}\left[\frac{3}{(k_0 r)^2} + j\frac{3}{k_0 r} - 1\right], \tag{2c}$$

$$g_2(r) = \frac{e^{-jk_0 r}}{r}\left[\frac{2}{(k_0 r)^2} + j\frac{2}{k_0 r}\right]. \tag{2d}$$

The equation (1) can be written as the following matrix:

$$\begin{bmatrix} a_{H_x}^{M_x} & a_{H_x}^{M_y} \\ a_{H_y}^{M_x} & a_{H_y}^{M_y} \\ a_{H_z}^{M_x} & a_{H_z}^{M_y} \end{bmatrix} \begin{bmatrix} M_x \\ M_y \end{bmatrix} = \begin{bmatrix} H_x \\ H_y \\ H_z \end{bmatrix}. \tag{3}$$

Letting the number of scanning points be *m* and the number of dipoles be *n* ($m \geq n$ is required), (3) can be written as:

$$\begin{pmatrix} a_{H_{1x}}^{M_{1x}} & a_{H_{1x}}^{M_{1y}} & \cdots & a_{H_{1x}}^{M_{nx}} & a_{H_{1x}}^{M_{ny}} \\ a_{H_{1y}}^{M_{1x}} & a_{H_{1y}}^{M_{1y}} & \cdots & a_{H_{1y}}^{M_{nx}} & a_{H_{1y}}^{M_{ny}} \\ a_{H_{1z}}^{M_{1x}} & a_{H_{1z}}^{M_{1y}} & \cdots & a_{H_{1z}}^{M_{nx}} & a_{H_{1z}}^{M_{ny}} \\ \vdots & \vdots & \ddots & \vdots & \vdots \\ a_{H_{mx}}^{M_{1x}} & a_{H_{mx}}^{M_{1y}} & \cdots & a_{H_{mx}}^{M_{nx}} & a_{H_{mx}}^{M_{ny}} \\ a_{H_{my}}^{M_{1x}} & a_{H_{my}}^{M_{1y}} & \cdots & a_{H_{my}}^{M_{nx}} & a_{H_{my}}^{M_{ny}} \\ a_{H_{mz}}^{M_{1x}} & a_{H_{mz}}^{M_{1y}} & \cdots & a_{H_{mz}}^{M_{nx}} & a_{H_{mz}}^{M_{ny}} \end{pmatrix}_{3m\times 2n} \begin{pmatrix} M_{1x} \\ M_{1y} \\ \vdots \\ M_{nx} \\ M_{ny} \end{pmatrix}_{2n} = \begin{pmatrix} H_{1x} \\ H_{1y} \\ H_{1z} \\ \vdots \\ H_{mx} \\ H_{my} \\ H_{mz} \end{pmatrix}_{3m}. \tag{4}$$

The equation (4) can also be simplified as:

$$AM = H, \tag{5}$$

where the matrix *A* can be obtained by the defined near-field sampling grids and dipole locations. The Tikhonov regularization method addressed in [8] is applied to deal with the ill condition problem, and the regularization parameters are obtained by generalized cross validation (GCV) method, which is the value of $\min \mathrm{GCV}(\lambda)$.

B. Numerical validation

Figure 1 (a) gives a patch antenna model, its physical structure is a 60mm×60mm×1mm board (Rogers RT substrate) with a circle patch (radius is 23mm) on one face and a ground plane on the other face, and the excitation source is 1V voltage through a coaxial cable. The antenna model is calculated with HFSS at its working frequency 2.5GHz, and the magnetic field data on the plane 10mm off the antenna's top surface is extracted. The size of the scanning plane is 80mm×80mm, scanning resolution is 4mm, and the total number of sampling points is 441.

The constructed equivalent model is as shown in Fig. 1 (b), consists of an initial matrix of 9×9 dipoles within an area of 48mm×48mm. Each dipole can be represented by two tangential moment components M_x and M_y.

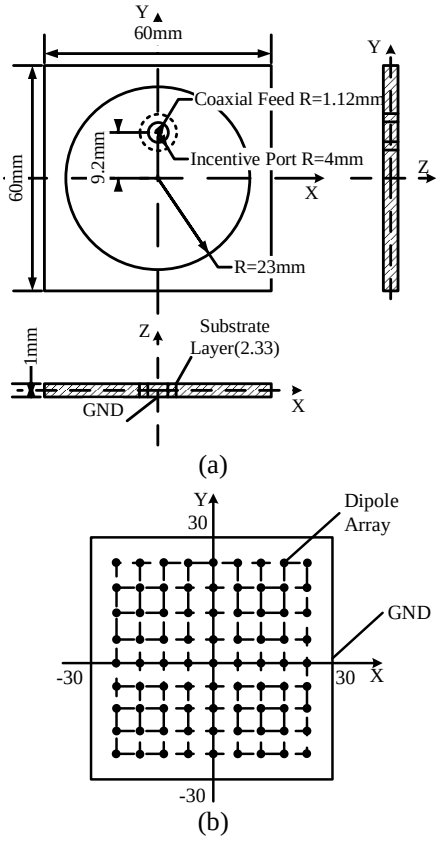

Fig. 1. (a) The physical structure of a patch antenna, and (b) the equivalent dipole array model of the antenna.

Importing the near-field data into MATLAB, the dipole moments are calculated by Tikhonov regularization method, Fig. 2 is the determination of regularization parameter (λ) by using GCV. Then equivalent model is obtained.

The magnetic fields on the plane 10mm above the upper surface of antenna from the original PCB and the equivalent model are compared in Fig. 3. It can be seen that the equivalent model can predict the radiating fields of the PCB quiet accurately, all the relative errors of each component calculated by (6), as summarized in Table 1, are smaller than 5%. It should be note that the relative error of H_x smaller than that of H_y and H_z is random. Actually, several attempts later we find that it will change with different near-field scanning and equivalent modeling parameters. Normally, we only need to consider that if the errors of H_x, H_y and H_z are smaller than 10%, then we think the equivalent model is available:

$$\sigma = \frac{\left|\sum_{m=1}^{M}\left|H_{im}^{means}\right| - \sum_{m=1}^{M}\sum_{n=1}^{N}\left|H_{im}^{model}\right|\right|}{\sum_{m=1}^{M}\left|H_{im}^{means}\right|} \quad i = x, y, z\,. \tag{6}$$

To extend the application of the equivalent modeling method, the following section will propose an improved analytical algorithm to enhance the efficiency of calculating board-level radio-frequency interference in [17].

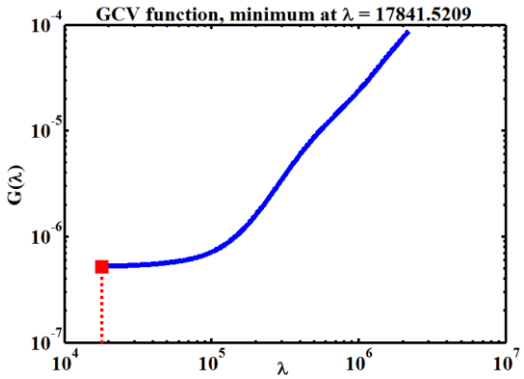

Fig. 2. Determination of regularization parameter by GCV.

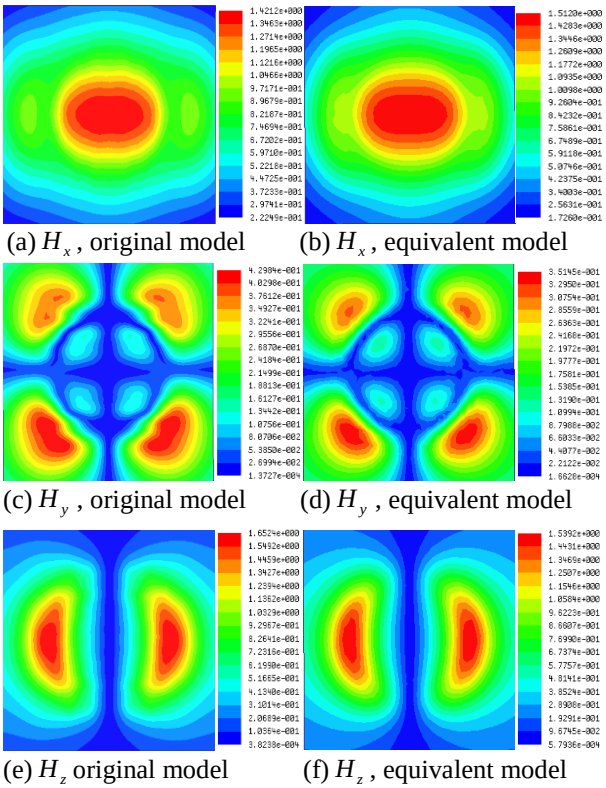

(a) H_x, original model (b) H_x, equivalent model

(c) H_y, original model (d) H_y, equivalent model

(e) H_z original model (f) H_z, equivalent model

Fig. 3. A comparison of magnetic field distribution between the original antenna model and the equivalent dipole model in free space by full-wave simulation.

Table 1: Relative errors of equivalent model

	H_x	H_y	H_z	H_{total}
10mm above the upper surface of PCB	0.58%	4.87%	4.49%	0.84%

III. RADIO-FREQUENCY INTERFERENCE ESTIMATION

A. Basic theory

According to [18], a decomposition method based on reciprocity theory is proposed to predict near-field coupling from a digital noise source to an RF antenna. This method consists of three main steps. Firstly, a Huygens' box is introduced to enclose the victim antenna, and the antenna is removed. Then, an equivalent dipole array model of working noise source is applied to calculate the tangential electromagnetic fields on the external surface of Huygens' box. This is a forward problem. Secondly, the victim antenna is excited, and the tangential electromagnetic fields on the internal surface of the same Huygens' box are recorded by using full-wave simulation. This is a reverse problem. Thirdly, the coupling parameter between noise source and victim antenna is calculated by the recorded tangential electromagnetic fields and reciprocity theory. Examples in [18] show that this method has achieved decent RFI estimation, but the calculation of the tangential electromagnetic fields is time-consuming in the second step. So the electromagnetic fields achieved by equivalent dipole model is proposed in this paper. This method can improve the calculating efficiency significantly with high accuracy, especially for antenna array where noise and victim sources share the same model. Then the original problem can be transformed into the equivalent problem as shown in Fig. 4, and the three main steps are described as follows.

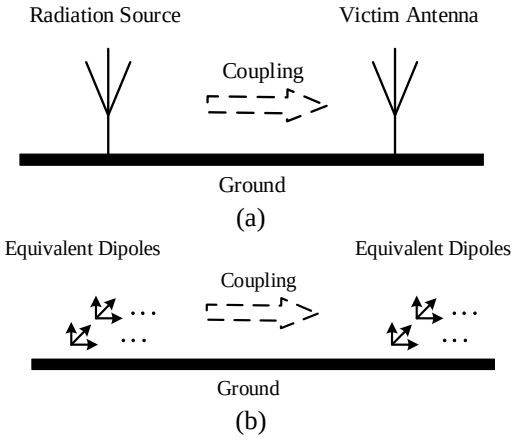

Fig. 4. (a) Original coupling problem, and (b) equivalent problem.

(1) Forward Problem: As shown in Fig. 5 (a), victim source is enclosed by Huygens' box, and then it is removed. Excite the noise source, and the induced electromagnetic fields on the port of noise source are named as E_a^{fwd}, H_a^{fwd}. Establish the equivalent dipole model of the noise source, and divide the surface of Huygens' box into small cells. Then the tangential electromagnetic field on each cell can be calculated by equivalent model, which named as E_c^{fwd}, H_c^{fwd}.

(*2) Reverse Problem*: Similar to step1, as illustrated in Fig. 5 (b), keep victim source being enclosed, remove the noise source, and excite the victim source instead. The excited electromagnetic fields are recorded as E_a^{rev}, H_a^{rev}. Then establish equivalent model of victim source, and calculate the tangential electromagnetic fields on the same cells, and they are named as E_c^{rev}, H_c^{rev}.

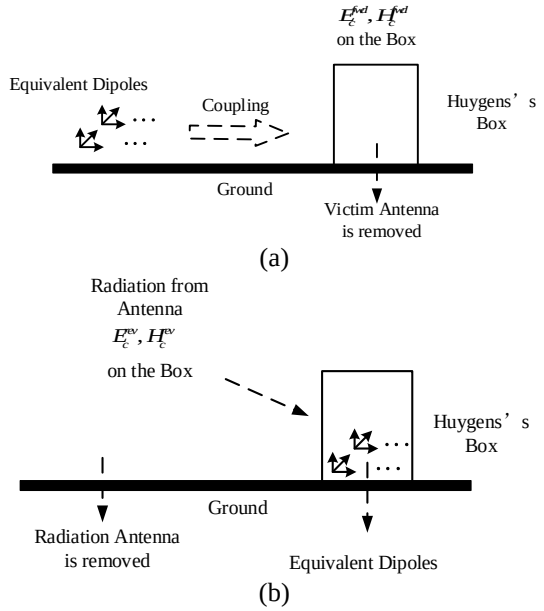

Fig. 5. (a) Forward problem, and (b) reverse problem.

(3) Interference Estimation: According to [18], based on the forward problem and reverse problem, the reciprocity theory can be expressed as:

$$\begin{aligned} &-\int_S \left(E^{rev}\times H^{fwd} - E^{fwd}\times H^{rev}\right)\cdot ds \\ &= \int_V \left(E^{rev}\times J^{fwd} + H^{fwd}\times M^{rev}\right) dv \\ &-\int_V \left(E^{fwd}\times J^{rev} + H^{rev}\times M^{fwd}\right) dv, \end{aligned} \tag{7}$$

where J and M represent the electric current and magnetic current source, respectively. "*fwd*" means the forward problem, and "*rev*" means the reverse problem. If equation (7) is integrated over the entire space, it can be simplified as:

$$\int_V \left(E_c^{rev}\cdot J_c^{fwd} - H_c^{rev}\cdot M_c^{fwd}\right)dv = \int_V \left(E_a^{fwd}\cdot J_a^{rev} - H_a^{fwd}\cdot M_a^{rev}\right)dv, \tag{8}$$

where subscript "*a*" means the antenna port, and "*c*" the electric/magnetic field and current on the Huygens' box. By dividing the Huygens' box into cells and replacing *J* and *M*: through electric field and magnetic field, the two terms on the left side of (8) are derived as:

$$\begin{aligned}\int_V \left(E_c^{rev}\cdot J_c^{fwd}\right)dv &= \int_{S_c}\left(E_c^{rev}\cdot J_c^{fwd}\right)ds \\ &= \sum_{cells} E_c^{rev}\cdot J_c^{fwd} S_{cell} \\ &= \sum_{cells} E_c^{rev}\cdot\left(\hat{n}\times H_c^{fwd}\right)S_{cell},\end{aligned} \tag{9}$$

$$\begin{aligned}\int_V \left(H_c^{rev}\cdot M_c^{fwd}\right)dv &= \int_{S_c}\left(H_c^{rev}\cdot M_c^{fwd}\right)ds \\ &= \sum_{cells} H_c^{rev}\cdot M_c^{fwd} S_{cell} \\ &= \sum_{cells} H_c^{rev}\cdot\left(E_c^{fwd}\times\hat{n}\right)S_{cell},\end{aligned} \tag{10}$$

where $\hat{n}$ is the normal vector of the cells, S_{cell} the area of a single cell. The right side of (8) can be written as [18]:

$$\int_V \left(E_a^{fwd}\cdot J_a^{rev}\right)dv = -\int_{S_a} E_a^{fwd}\cdot J_a^{rev}ds = -I_a^{rev}U_a^{fwd}, \tag{11}$$

$$\begin{aligned}\int_V \left(H_a^{fwd}\cdot M_a^{rev}\right)dv &= \int_V H_a^{fwd}\cdot\left(E_a^{rev}\times\hat{n}\right)dv \\ &= \int_V E_a^{rev}\cdot\left(\hat{n}\times H_a^{fwd}\right)dv \\ &= \int_V E_a^{rev}\cdot J_a^{fwd}dv \\ &= \int_{S_a} J_a^{fwd}E_a^{rev}ds = I_a^{fwd}U_a^{rev}.\end{aligned} \tag{12}$$

Substituting (9)-(12) into (8), we obtain:

$$\begin{aligned}&\sum_{cells}\hat{n}\times H_c^{fwd}\cdot E_c^{rev}S_{cell} + \sum_{cells}\hat{n}\times E_c^{fwd}\cdot H_c^{rev}S_{cell} \\ &= -I_a^{rev}U_a^{fwd} - I_a^{fwd}U_a^{rev} \\ &= -\frac{Z_{in}+Z_L}{Z_{in}Z_L}U_a^{fwd}U_a^{rev},\end{aligned} \tag{13}$$

where Z_{in} and Z_L are respectively the input impedance of the victim source and the load of the noise source, 50Ω in common. U_a^{rev} is the excitation voltage of the victim source, and here is 1V. Thus, the coupling voltage can be solved as:

$$\begin{aligned}U_a^{fwd} &= -\frac{Z_{in}Z_L}{U_a^{rev}(Z_{in}+Z_L)} \\ &\times\left(\sum_{cells}\hat{n}\times H_c^{fwd}\cdot E_c^{rev}S_{cell} + \sum_{cells}\hat{n}\times E_c^{fwd}\cdot H_c^{rev}S_{cell}\right).\end{aligned} \tag{14}$$

Assuming that U_{in} is the incident voltage of noise source, the scattering parameter can be calculated by (15):

$$\begin{aligned}S &= \frac{U_a^{fwd}}{U_{in}} \\ &= -\frac{Z_{in}Z_L}{U_a^{rev}U_{in}(Z_{in}+Z_L)} \\ &\times\left(\sum_{cells}\hat{n}\times H_c^{fwd}\cdot E_c^{rev}S_{cell} + \sum_{cells}\hat{n}\times E_c^{fwd}\cdot H_c^{rev}S_{cell}\right).\end{aligned} \tag{15}$$

B. Numerical validation

As illustrated in Fig. 6, a patch antenna array model is constructed with four antenna elements which are the same as that in Section II. Assuming that Part 1 is the noise source, Part 2, 3, 4 are the victim sources. A 60mm×60mm×60mm Huygens' box is applied to enclose the victim sources, then its surface is divided into small cells with a size of 1mm×1mm. Based on the equivalent dipole model of the single patch antenna in Section II, both the tangential electromagnetic fields on the Huygens' box in the forward problem (E_a^{fwd} , H_a^{fwd}) and reverse problem (E_c^{rev} , H_c^{rev}) can be calculated from the dipoles.

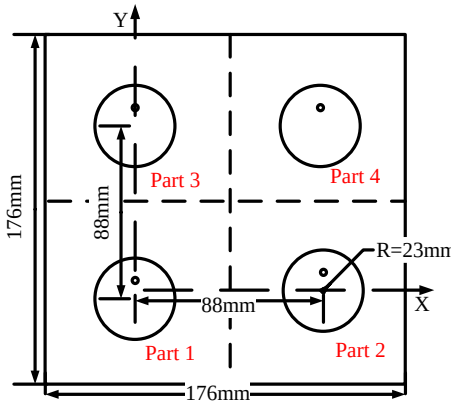

Fig. 6. Patch antenna array structure.

Substituting all the data into (14) and (15), the scattering parameters are calculated. Figure 7 shows the comparison of the scattering parameters between the proposed method and HFSS simulation. Note that part 2 and part 3 share the same scattering parameter because of their symmetry. It can be seen that the proposed method can predict the scattering parameters well. Thus, the worst coupling frequency (2.5 GHz, it is both the frequency point corresponding to the peak of scattering parameters and the working frequency of patch antenna) could be identified with high efficiency, and the precision of equivalent dipole model is further validated.

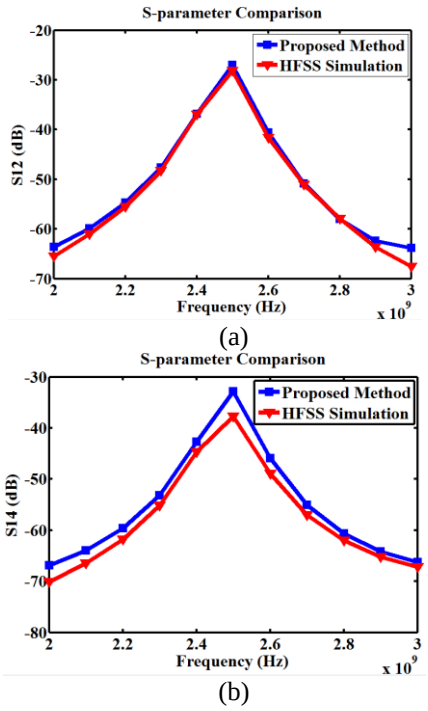

Fig. 7. Comparison of scattering parameters: (a) S_{12} and (b) S_{14} .

IV. ELECTROMAGNETIC LEAKAGE ESTIMATION

This section will verify the estimation accuracy of electromagnetic leakage with our equivalent dipole model. Figure 8 (a) shows an M micro-strip line which is a common trace structure on a PCB. Applying the method described in Section II, its equivalent dipole model is established as illustrated in Fig. 8 (b).

Place respectively the original micro-strip line model and its equivalent model into a shielding cavity with aperture arrays, and calculate these two models by HFSS at 1GHz. The cavity's size is 240mm×60mm×200mm, and 12 apertures are uniformly distributed on one face of the cavity, and other details of the cavity and aperture arrays are shown in Fig. 9.

Figure 10 demonstrates the HFSS simulation results of the magnetic field at 1GHz on the plane 3mm above the aperture face (outside of the cavity) from these two models, and the relative errors are summarized in Table 2. It can be seen that the equivalent dipole model can predict the electromagnetic leakage with acceptable errors (smaller than 10%), which depicts that the equivalent model is applicable to describe the interaction between the original PCB model and the enclosure. On the other hand, the results in a half-closed environment are slightly worse than in free place, because multiple reflection of electromagnetic fields in cavity may change real current distribution on PCB, and make the error of equivalent model bigger.

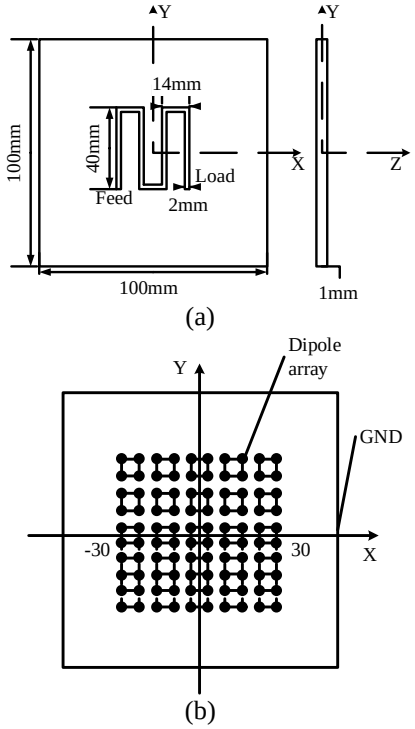

Fig. 8. (a) Physical structure of M micro-strip line, and (b) equivalent dipole array model of micro-strip line

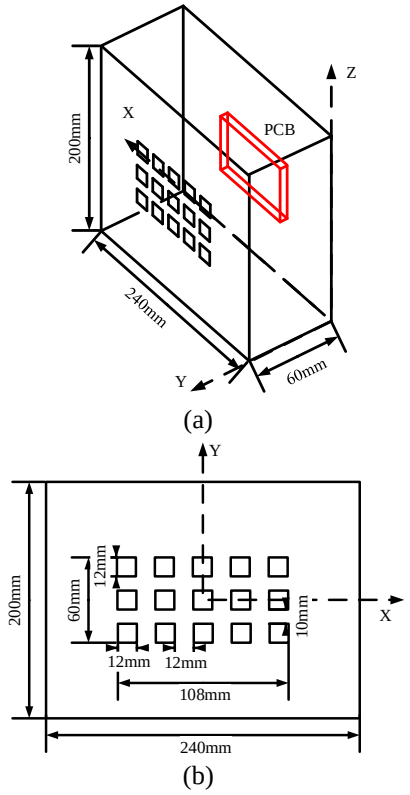

Fig. 9. (a) Structure of shielding cavity, and (b) structure of aperture face.

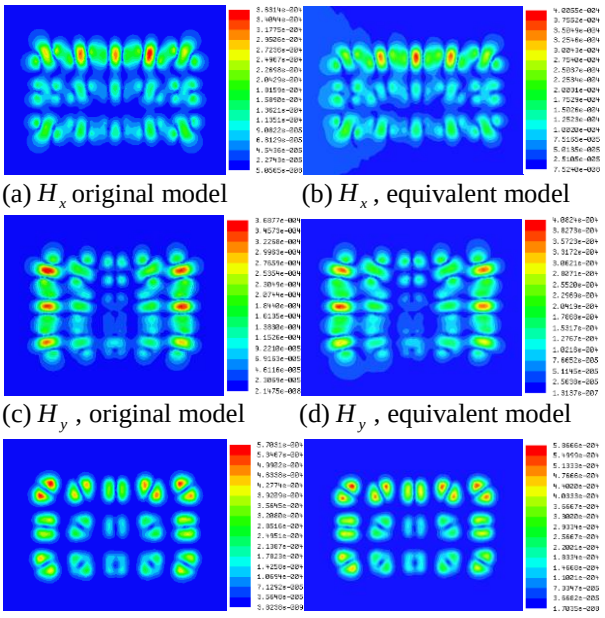

(a) H_x original model (b) H_x, equivalent model

(c) H_y, original model (d) H_y, equivalent model

(e) H_z, original model (f) H_z, equivalent model

Fig. 10. Magnetic field distribution comparison between original antenna model and equivalent dipole model in aperture array cavity by full-wave simulation.

Table 2: Relative errors of equivalent model

	H_x	H_y	H_z	H_{total}
3mm above the aperture face (outside) of PCB	9.33%	3.94%	6.57%	5.07%

V. CONCLUSION

This paper proposes an equivalent dipole modeling method of a PCB. This method can model original PCB emission characteristics when its physical structure and circuit structure are uncertain or complicated, and can be applied in some common structures like board-level patch antenna, micro-strip line, and other complicated IC structures. An improved analytical algorithm of board-level electromagnetic coupling estimation is also proposed using the equivalent dipole modeling method and reciprocity theory. Compared with full-wave simulation, the proposed method can predict the electromagnetic coupling parameters and the worst coupling frequency fast, especially when the structure of noise source is the same as that of victim source like the patch antenna array. Then, the application of equivalent dipole model is extended to predict the electromagnetic leakage of a PCB in an enclosure with numerous small apertures, and the calculation precision is validated by a common micro-strip line model. Finally, the limitation of the proposed equivalent method is that it only applies to relative lower frequency (smaller than 4GHz). Because with an increase of the frequency, the number of the equivalent dipole increases and the relative errors also become greater. However, with emergence of higher frequency electronic equipment, further work can be done to explore the equivalent model of PCB in these kind of devices. Besides, method to decrease the relative errors of equivalent model in half enclosed cavity also can be further taken into consideration.

ACKNOWLEDGMENT

This work is supported by the National Natural Science Foundation of China (Grant No. 51675086).

REFERENCES

[1] S. Deng, T. H. Hubing, and D. G. Beetner, "Using TEM cell measurements to estimate the maximum radiation from PCBs with cables due to magnetic field coupling," [J]. *IEEE Transactions on Electromagnetic Compatibility*, vol. 50, no. 2, pp. 419-423, 2008.

[2] B. L. Nie, P. A. Du, Y. T. Yu, et al., "Study of the shielding properties of enclosures with apertures at higher frequencies using the transmission-line modeling method," [J]. *IEEE Transactions on Electromagnetic Compatibility*, vol. 53, no. 1, pp. 73-81, 2011.

[3] P. Xiao, P. A. Du, D. Ren, et al., "A hybrid method for calculating the coupling to PCB inside a nested shielding enclosure based on electromagnetic topology," [J]. *IEEE Transactions on Electromagnetic Compatibility*, vol. 58, no. 6, pp. 1701-1709, 2016.

[4] P. Xiao, P. A. Du, B. L. Nie, et al., "Reduced technique for modeling electromagnetic immunity on braid shielding cable bundles," [J]. *Chinese Physics B*, vol. 26, no. 9, pp. 175-183, 2017.

[5] J. Shi, M. A. Cracraft, J. Zhang, et al., "Using near-field scanning to predict radiated fields," [C]. *International Symposium on Electromagnetic Compatibility, IEEE*, vol. 1, pp. 14-18, 2004.

[6] H. Weng, D. G. Beetner, and R. E. Dubroff, "Prediction of radiated emissions using near-field measurements," [J]. *IEEE Transactions on Electromagnetic Compatibility*, vol. 53, no. 4, pp. 891-899, 2011.

[7] X. Tong, D. W. P. Thomas, et al., "Reduction of sensitivity to measurement errors in the derivation of equivalent models of emission in numerical computation," [J]. *Applied Mathematics & Computation*, vol. 26, no. 7, pp. 603-610, 2011.

[8] X. Tong, *Ph.D. dissertation*, United Kingdom: the University of Nottingham, 2010.

[9] X. Tong, D. W. P. Thomas, A. Nothofer, et al., "Modeling electromagnetic emissions from printed circuit boards in closed environments using equivalent dipoles," [J]. *IEEE Transactions on Electro-*

magnetic Compatibility, vol. 52, no. 2, pp. 462-470, 2010.

[10] C. Obiekezie, D. W. P. Thomas, A. Nothofer, et al., "Prediction of emission from a source placed inside a metallic enclosure over a finite ground plane," [C]. *International Symposium on Electromagnetic Compatibility, IEEE*, pp. 1-5, 2012.

[11] C. Obiekezie, D. W. Thomas, A. Nothofer, et al., "Extended scheme using equivalent dipoles for characterizing edge currents along a finite ground plane," [J]. *Applied Mathematics & Computation*, vol. 28, no. 11, pp. 1111-1121, 2013.

[12] F. P. Xiang, E. P. Li, X. C. Wei, et al., "A particle swarm optimization-based approach for predicting maximum radiated emission from PCBs with dominant radiators," [J]. *IEEE Transactions on Electromagnetic Compatibility*, vol. 57, no. 5, pp. 1197-1205, 2015.

[13] Z. Yu, J. A. Mix, S. Sajuyigbe, et al., "An improved dipole-moment model based on near-field scanning for characterizing near-field coupling and far-field radiation from an IC," [J]. *IEEE Transactions on Electromagnetic Compatibility*, vol. 55, no. 1, pp. 97-108, 2013.

[14] Z. Yu, J. A. Mix, S. Sajuyigbe, et al., "Heat-sink modeling and design with dipole moments representing IC excitation," [J]. *IEEE Transactions on Electromagnetic Compatibility*, vol. 55, no. 1, pp. 168-174, 2013.

[15] J. Zhang, D. Pommerenke, and J. Fan, "Determining equivalent dipoles using a hybrid source-reconstruction method for characterizing emissions from integrated circuits," [J]. *IEEE Transactions on Electromagnetic Compatibility*, vol. 59, no. 2, pp. 567-575, 2017.

[16] J. Pan, L. Li, X. Gao, et al., "Application of dipole-moment model in EMI estimation," [C]. *IEEE International Symposium on Electromagnetic Compatibility, IEEE*, pp. 350-354, 2015.

[17] H. Wang, V. Khilkevich, Y. J. Zhang, et al., "Estimating radio-frequency interference to an antenna due to near-field coupling using decomposition method based on reciprocity," [J]. *IEEE Transactions on Electromagnetic Compatibility*, vol. 55, no. 6, pp. 1125-1131, 2013.

[18] J. Pan, H. Wang, X. Gao, et al., "Radio-frequency interference estimation using equivalent dipole-moment models and decomposition method based on reciprocity," [J]. *IEEE Transactions on Electromagnetic Compatibility*, vol. 58, no. 1, pp. 75-84, 2016.

[19] J. D. Jackson, *Classical Electrodynamics*. [M]. J. Wiley, 1998.

Yin-Shuang Xiao was born in Chongqing, China, in 1991. She received the Bachelor of Industrial Engineering degree from UESTC, Chengdu, China, in 2014. She is currently a Master student at UESTC. Her research interests are electromagnetic compatibility (EMC), computational electromagnetic (CEM), multi-conductor transmission line (MTL), etc.

Dan Ren was born in Huainan, Anhui Province, China, in 1986. He received the doctoral degree of Mechanical Engineering from UESTC, Chengdu, China, in 2017. He is currently a Research Assistant at Institute of Electronic Engineering, China Academy of Engineering Physics. His research interests include numerical computation, electromagnetic measurement, electromagnetic simulation and High Power Microwave.

Pei Xiao was born in Shaoyang, Hunan Province, China, in 1989. He received the Bachelor of Industrial Engineering degree from UESTC, Chengdu, China, in 2013. He is currently a Ph.D. student at UESTC. His research interests are numerical computation, theoretical electromagnetic analysis including the EMT method, and EMC/EMI in Multi-conductor transmission line (MTL).

Ping-An Du received the M.S. and Ph.D degrees in Mechanical Engineering from Chongqing University, Chongqing, China, in 1989 and 1992, respectively. He is currently a Full Professor of Mechanical Engineering at the University of Electronic Science and Technology of China, Chengdu, China. His research interests include numerical simulation in EMI, vibration, temperature, and so on.